Electronic Supporting Information

L-Phenylalanine derived pseudopeptidic bioinspired materials: Zn (II) induced fluorescence enhancement and precise tuning of self-assembled nanostructures

Kamlesh Kumar Nigam, Arpna Tamrakar and Mrituanjay D. Pandey*

Department of Chemistry, Institute of Science, Banaras Hindu University, Varanasi- 221005

UP, India. Email: mdpandey.chem@bhu.ac.in

Fig. S1. ^{1}H NMR (500 MHz, CDCl$_3$) of **1**

Fig. S2. ^{13}C{^{1}H} NMR (126 MHz, CDCl$_3$) of **1**
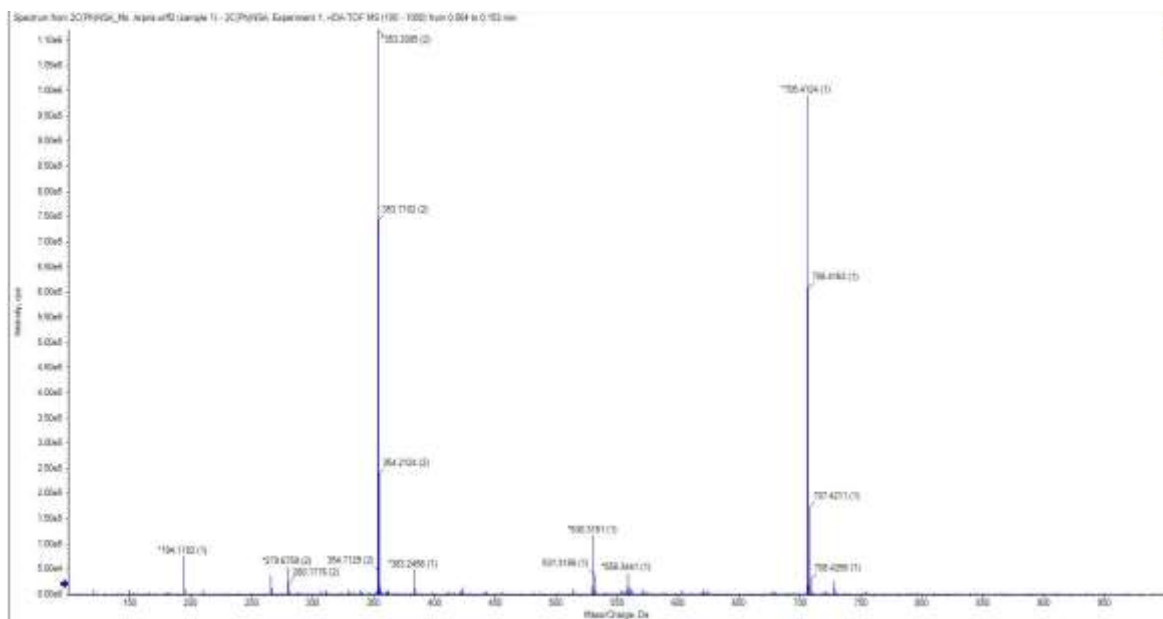
Fig. S3. HRMS data of **1**
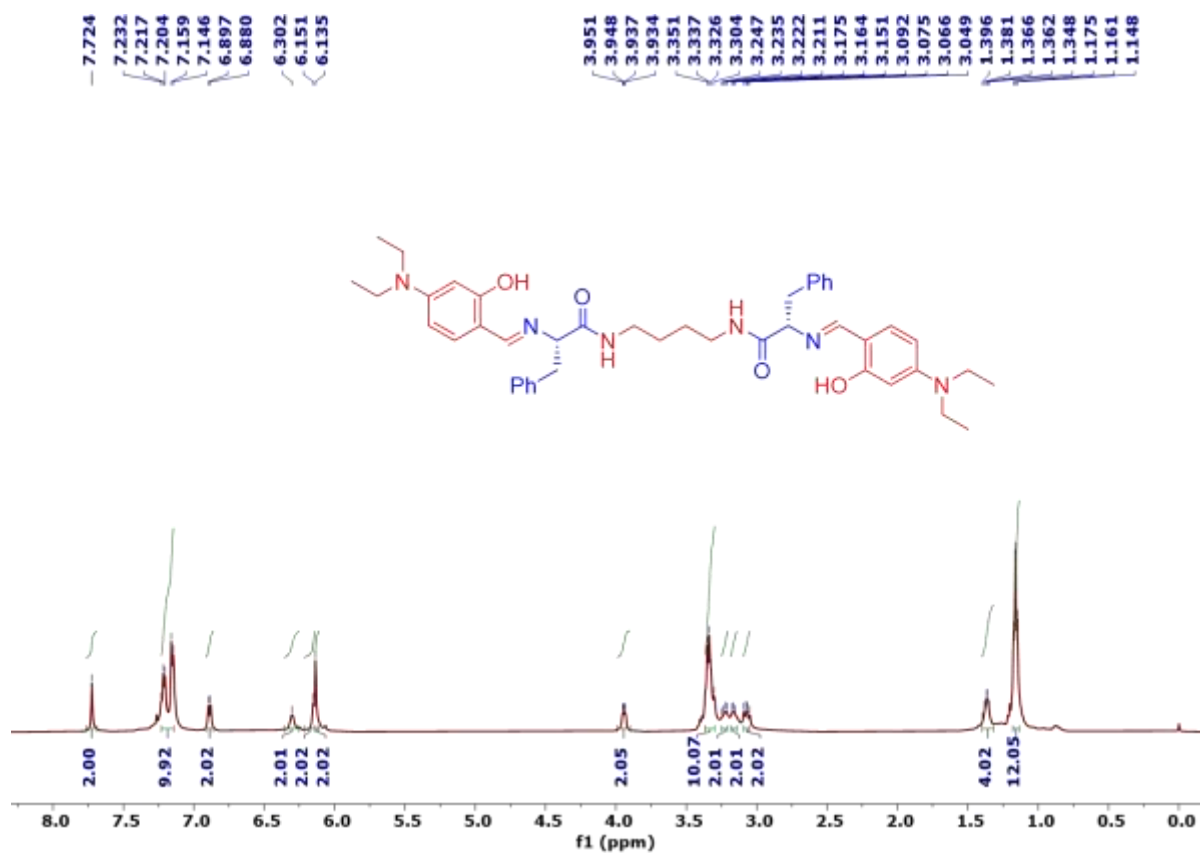
Fig. S4 ^{1}H NMR (500 MHz, CDCl$_3$) of **2**
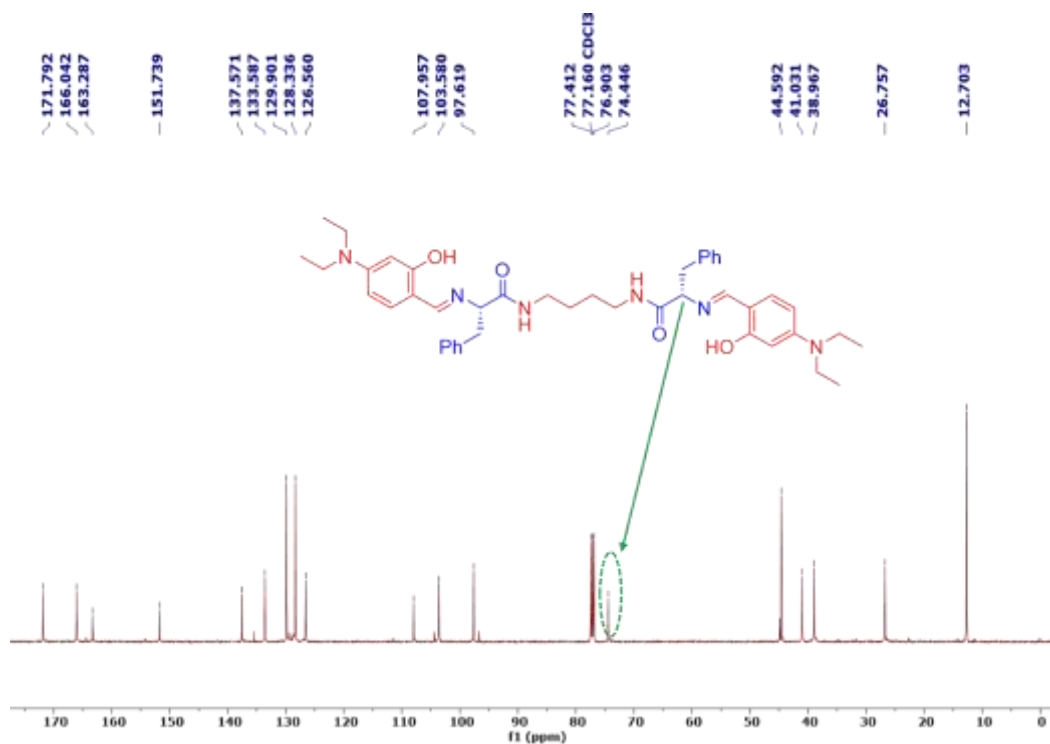
Fig. S5 $^{13}C\{^{1}H\}$ NMR (126 MHz, CDCl$_3$) of **2**
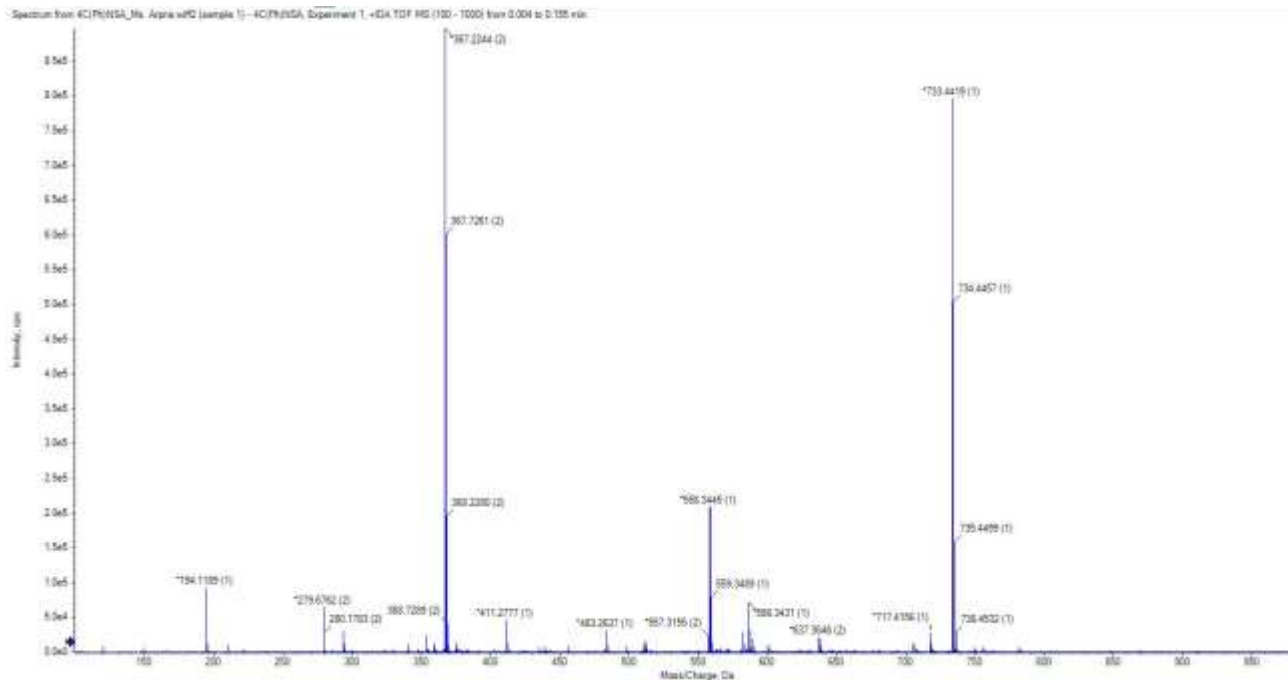
Fig. S6. HRMS data of **2**
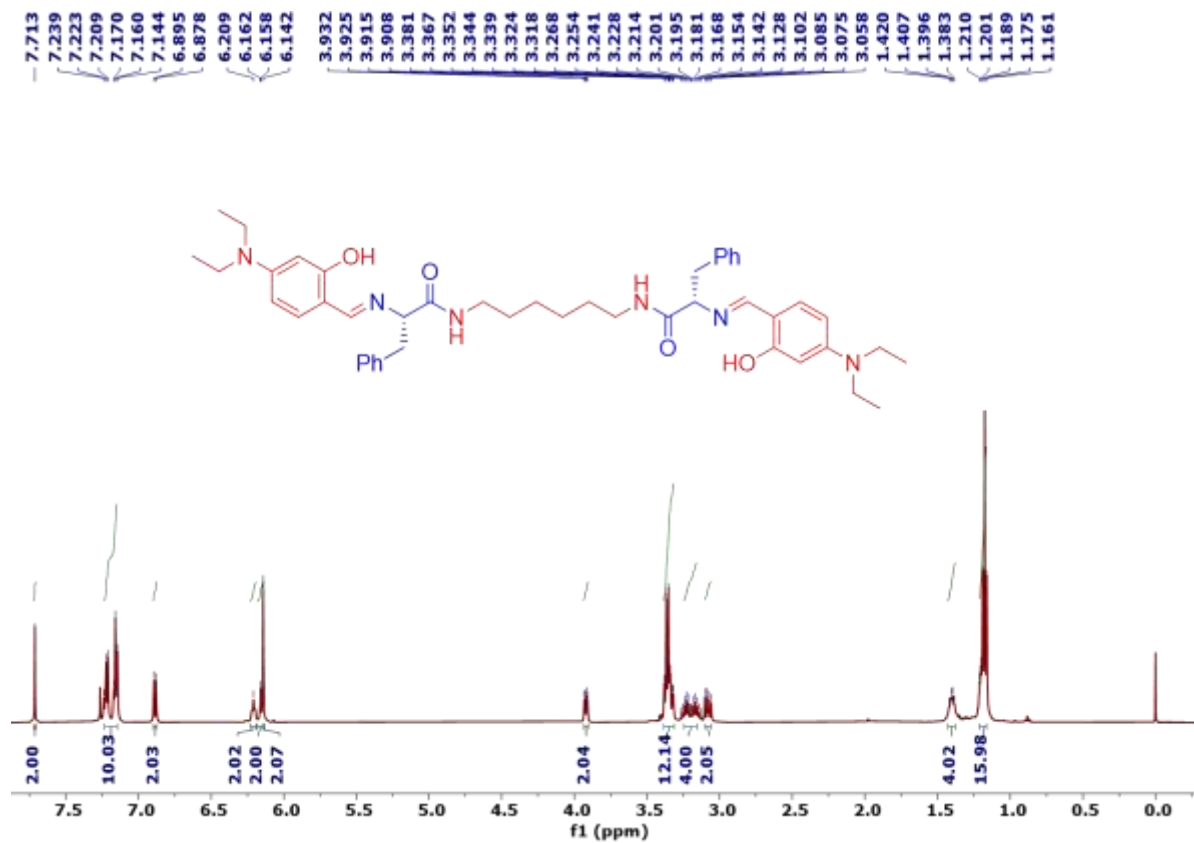
Fig. S7 ^{1}H NMR (500 MHz, CDCl$_3$) of **3**
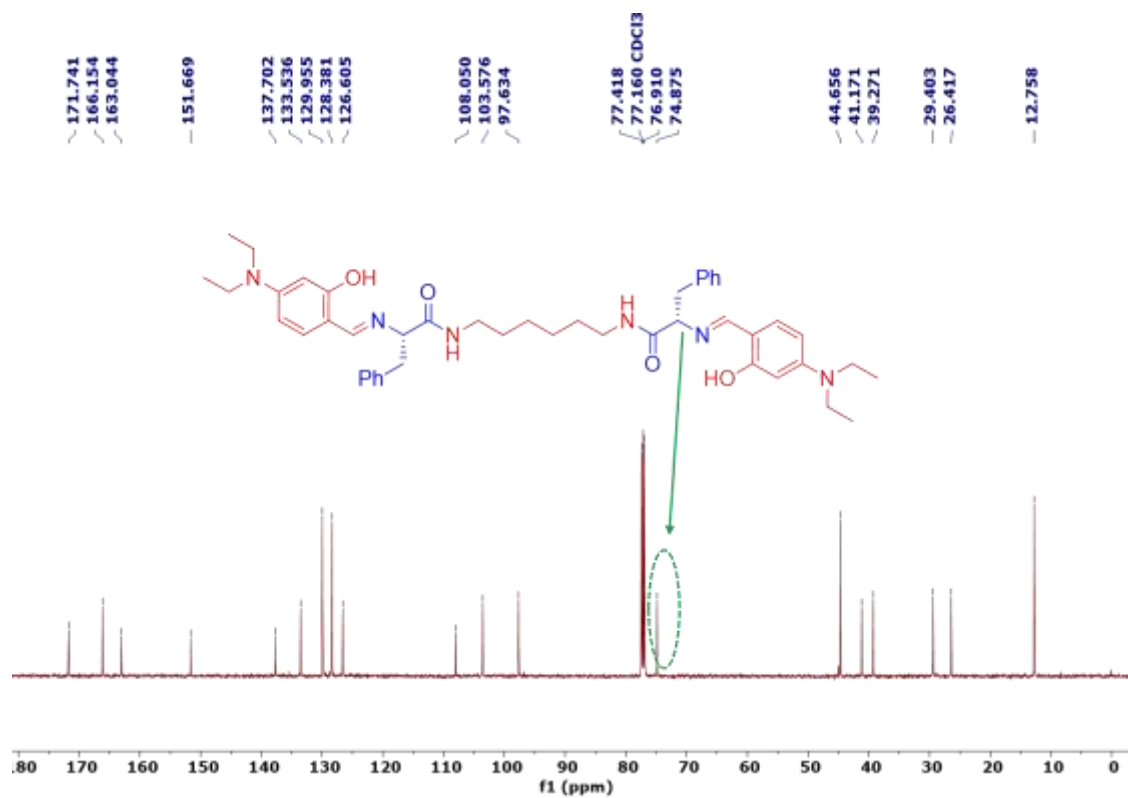
Fig. S8 ^{13}C{^{1}H} NMR (126 MHz, CDCl$_3$) of **3**
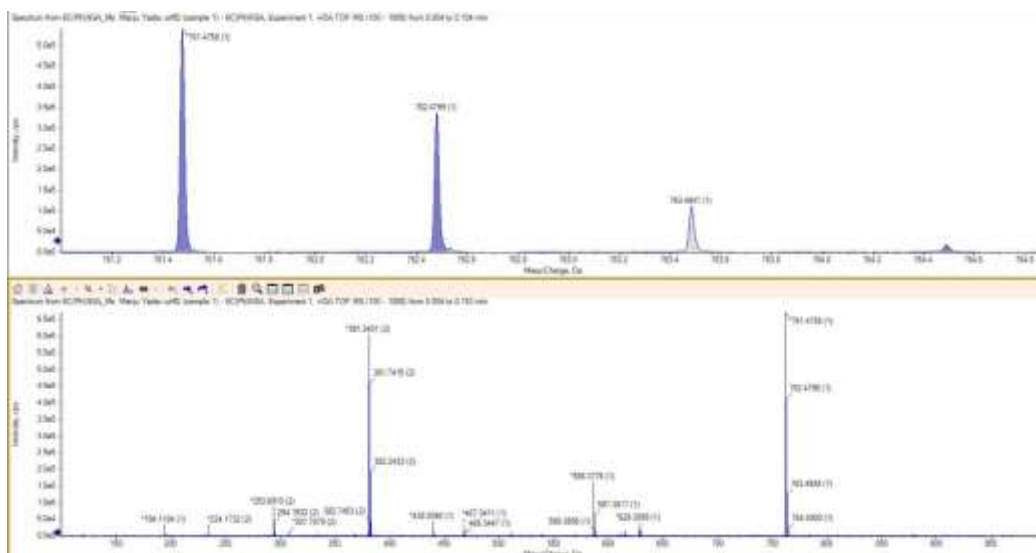
Fig. S9. HRMS data of **3.**
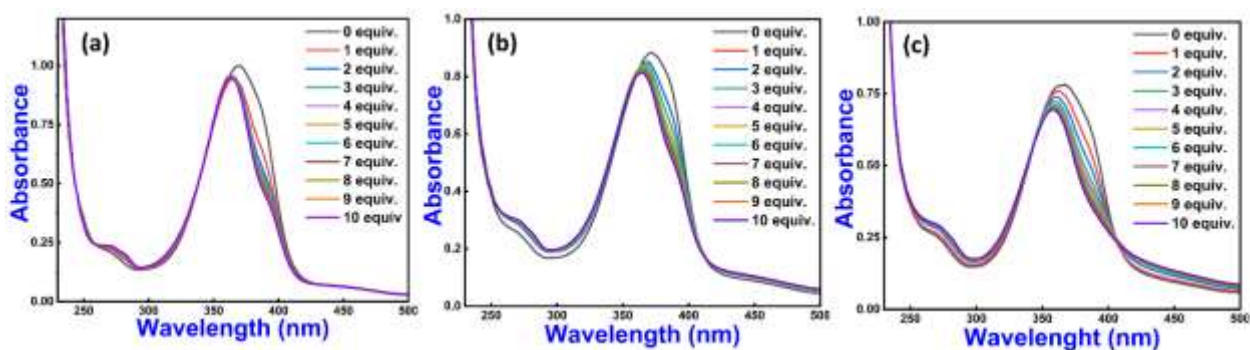
Fig. S10. UV-vis spectrum of **1** (a), **2** (b), and **3** (c) with increasing concentration of Zn(II) in HEPES

buffer (Water: ethanol = 3:7 v/v, 10μM; pH ~ 7.4).
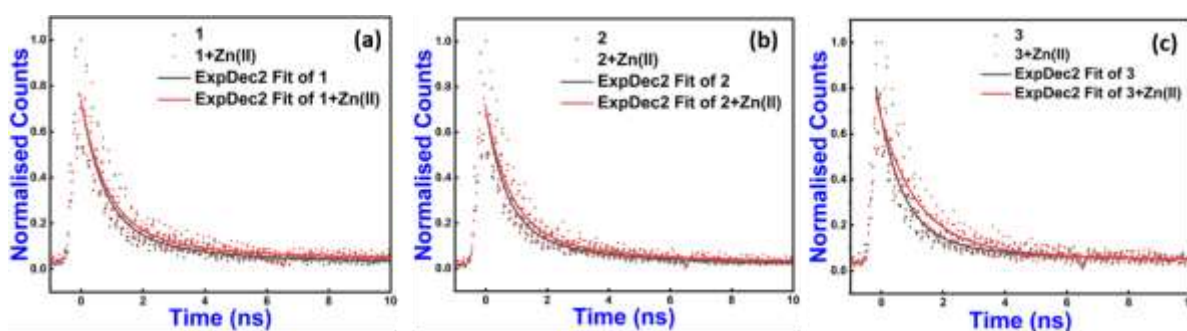
Fig. S11. Fluorescence average lifetime decay curve of **1** (10μM) and **1**-Zn(II) (10 equiv. of

Zn(II)) (a), **2** (10μM) and **2**-Zn(II) (10 equiv. of Zn(II)) (b), and **3** (10μM) and **3**-Zn(II) (10

equiv. of Zn(II)) (c) in HEPES buffer (Water: ethanol = 3:7 v/v, 10μM; pH ~ 7.4).
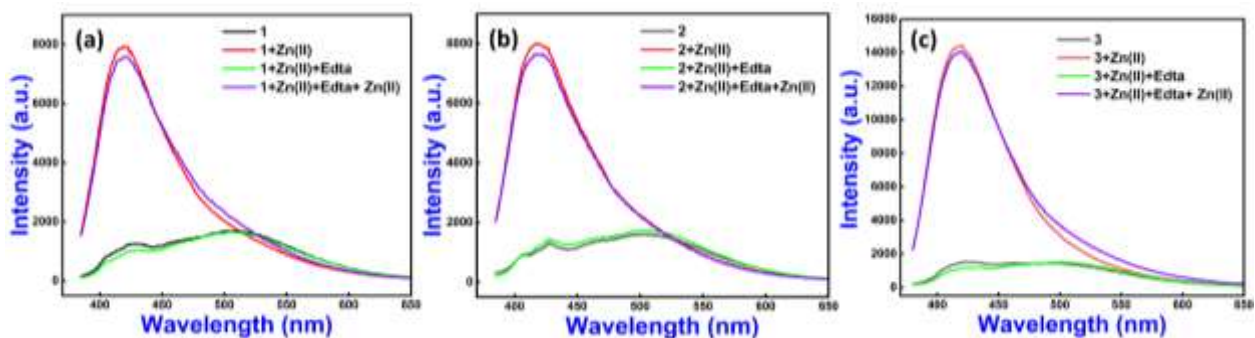
Fig. S12 Reversibility study of **1**-Zn(II) (a), **2**-Zn(II) (b) and **3-**Zn(II) (c) with EDTA.
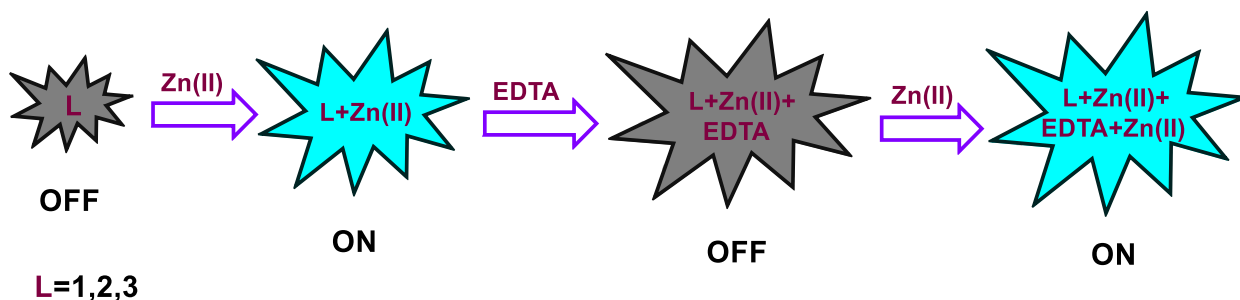
Fig. S13 Proposed model of reversibility for **1**-Zn(II), **2**-Zn(II) and **3**-Zn(II) with EDTA
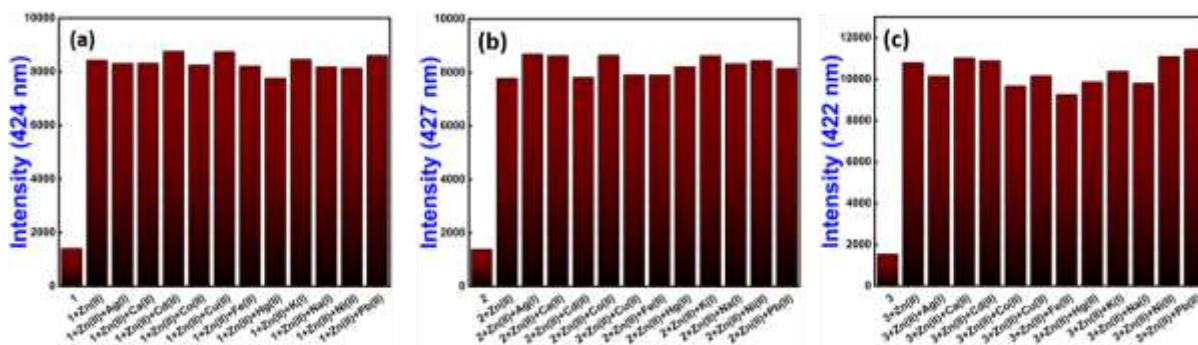
Fig. S14 Interference experiments of **1** (a), **2** (b), and **3** (c) with Zn(II) in presence of other competitive metal ions (at 424 nm, 427 nm, and 422 nm).

Binding stoichiometry and association constant

We conducted a jobs plot experiment to understand the binding stoichiometry of **1**-Zn(II), **2**-Zn(II), and **3-**Zn(II) systems. The jobs plot experiment from emission data displays

1:1 binding stoichiometry between **1-3** and Zn(II) ion (Figure S15). The association constant was calculated by using the Benesi-Hildebrand equation, i.e.

$$1/I\text{-}I_0 = 1/\ Ka\ [Zn(II)]\ [Imax - I_0] + 1/\ Imax\ \text{-}I_0,$$
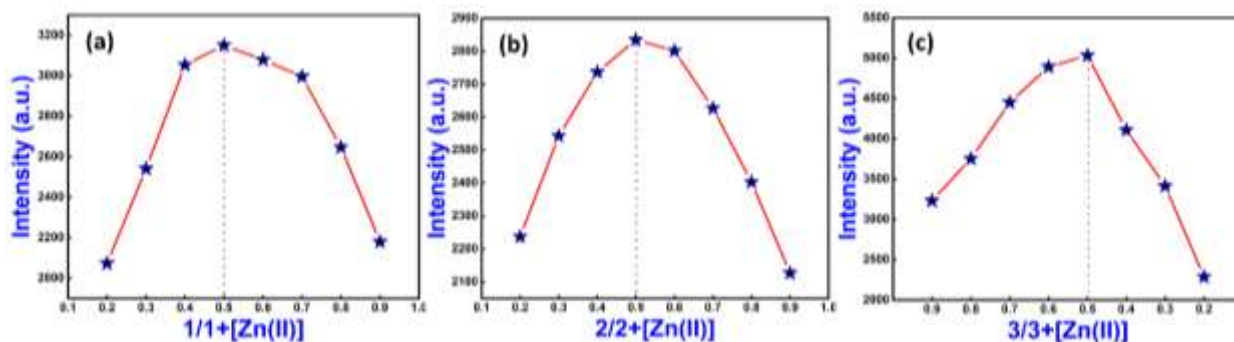
Fig. S15. Jobs plot study of **1**-Zn(II) (a), **2**-Zn(II) (b) and **3-**Zn(II) (c) (at 424 nm, 427 nm, and 422 nm) from emission spectra.

where I_0 indicates the emission intensity of neat **1-3** and I indicate the emission intensity of **1**-Zn(II), **2**-Zn(II) and **3-**Zn(II) system (variable with Zn(II) ion concentration), whereas, I_{max} indicates the emission intensity of **1**-Zn(II), **2**-Zn(II) and **3-**Zn(II) system at the maximum concentration of Zn(II) ion. The association constant (Ka) was obtained by plot between $1/(I\text{-}I_0)$ vs. $1/[Zn(II)]$ and found the value of Ka; 2.0×10^3 M^{-1} for **1-**Zn(II), 3.0×10^3 M^{-1} for **2-**Zn(II) and 1.1×10^3 M^{-1} for **3-**Zn(II) system. (Figure S16).
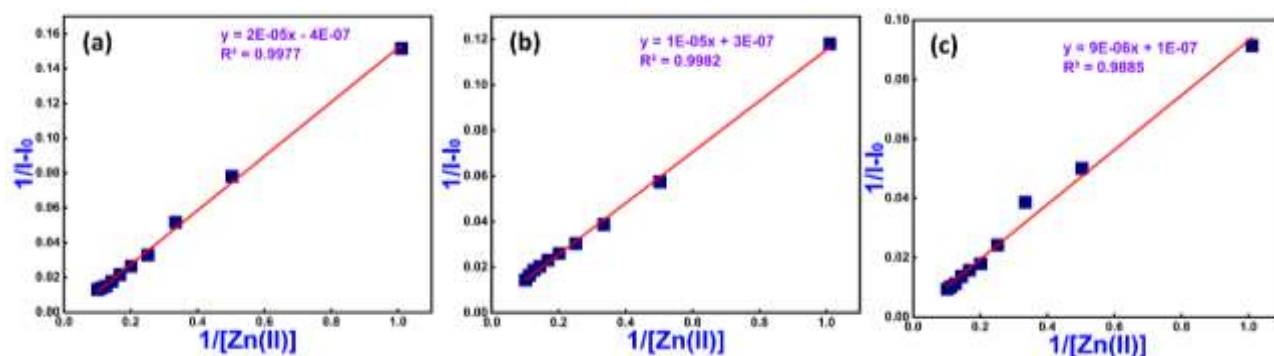
Fig. S16 Benesi-Hildebrand plot of **1**(a)**, 2**(b)**,** and **3**(c) emission spectra.

To measure the sensitivity of **1-3** toward Zn(II) ion, the varying concentration of Zn(II) (10^{-2} M – 10^{-12} M) were added to the solution of **1-3** (10 µM). A graph between fluorescence

intensity and concentration exhibits significant change at 10^{-6} M, 10^{-7} M, and 10^{-8} M concentrations of Zn(II) for **1**-Zn(II), **2**-Zn(II), and **3**-Zn(II) systems, respectively (Figure S17). For better accuracy, 10^{-6} M (1×10^{-6} M - 9×10^{-6} M), 10^{-7} M (1×10^{-7} M - 9×10^{-7} M), and 10^{-8} M (1×10^{-8} M - 9×10^{-8} M) of Zn(II) ion were added to the solution of **1-3** (10 µM), respectively and established the accurate limit of detection (LOD) values at 8.17×10^{-6} M or (0.534 ppm) for **1**-Zn(II), 8.28×10^{-7} M or (0.054 ppm) for **2**-Zn(II) and 8.31×10^{-8} M or (0.005 ppm) for **3**-Zn(II) system (Figure S18) by applying the formula 3σ/S where σ indicate the standard deviation of neat **1-3** and S indicate the slope from the plot between the concentration of sample and emission intensity.
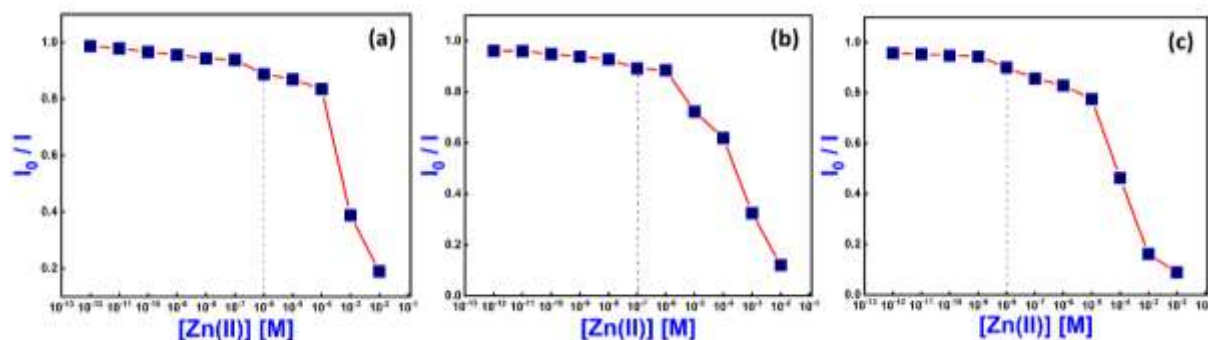
Fig. S17 Sensitivity plots of **1**(a)**, 2**(b)**,** and **3**(c) with different concentration of Zn(II) ion (10^{-2} – 10^{-12} M) from emission spectra.
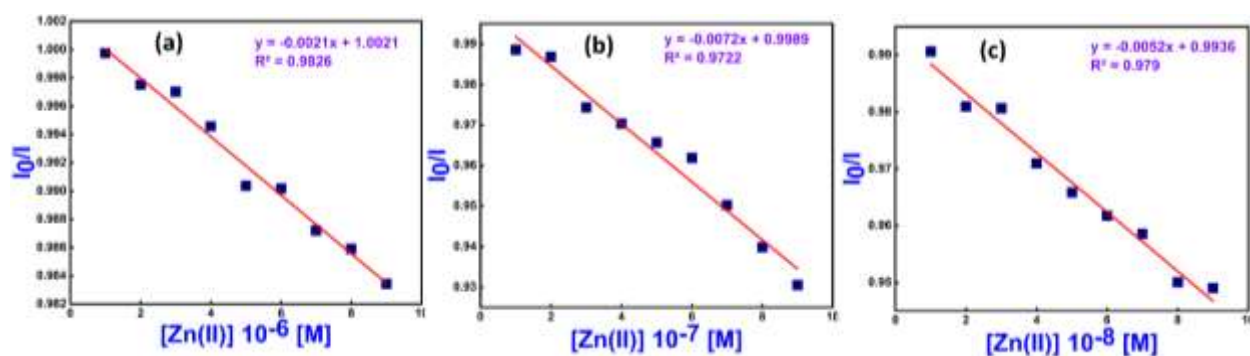
Fig. S18 LOD plots of **1** (a), **2** (b), and **3** (c) with different concentration of Zn(II) ion (1×10^{-6} M to 9×10^{-6} M for **1**, 1×10^{-7} M to 9×10^{-7} M for **2** and 1×10^{-8} M to 9×10^{-8} M for **3**) via; emission spectra.
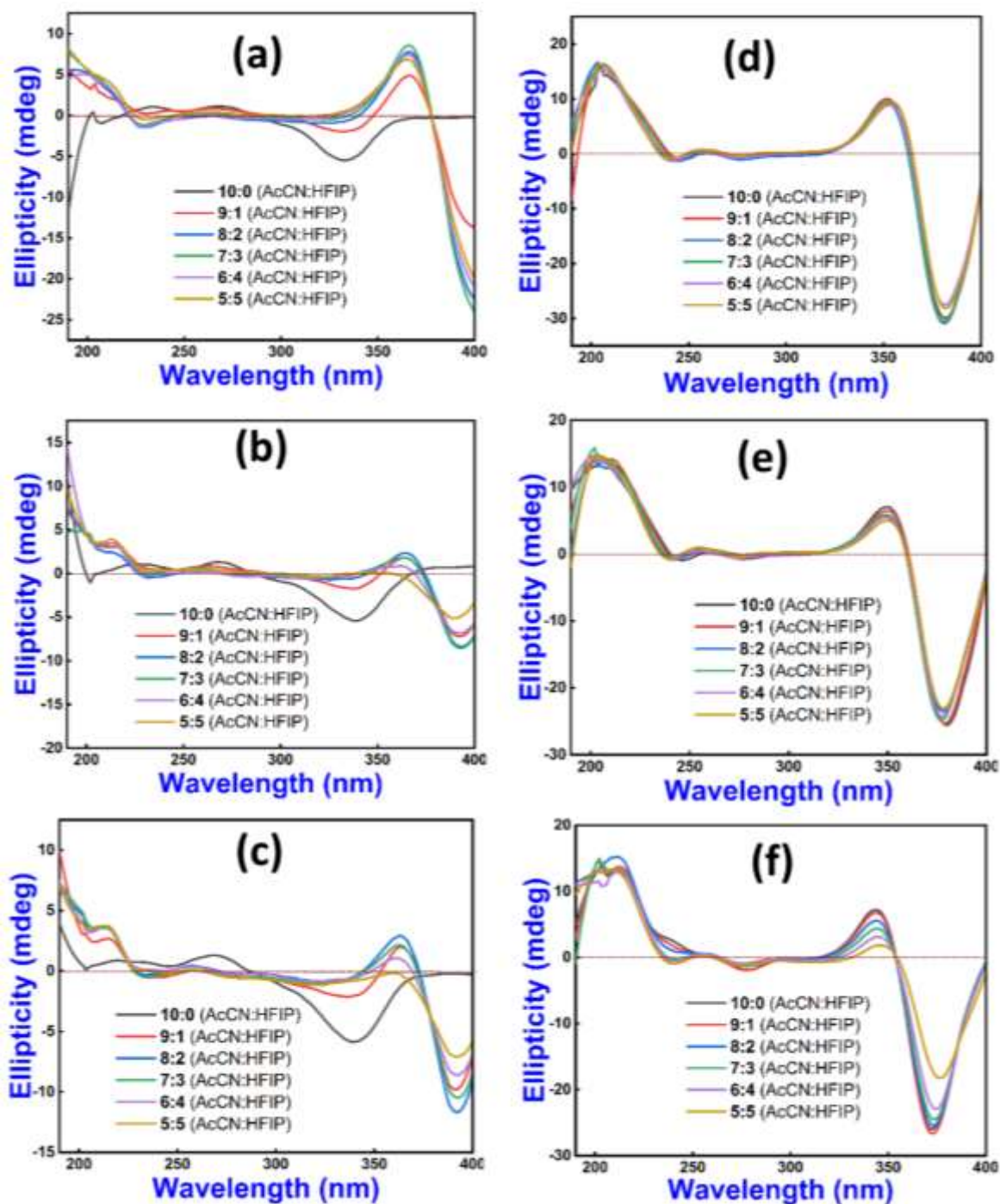
Fig. S19A. Circular Dichroism (CD) spectra of **1** (a), **2** (b), **3** (c) and **1-**Zn(II) (d), **2-**Zn(II) (e), **3-**Zn(II) (f), in different solvent combination of Acetonitrile and Hexafluoro isopropanol (HFIP) (AcCN:HFIP; v/v, 10:0 (Black line), 9:1 (Red line), 8:2 (Blue line), 7:3 (Green line), 6:4 (Voilet line), 5:5 (Yellow line))
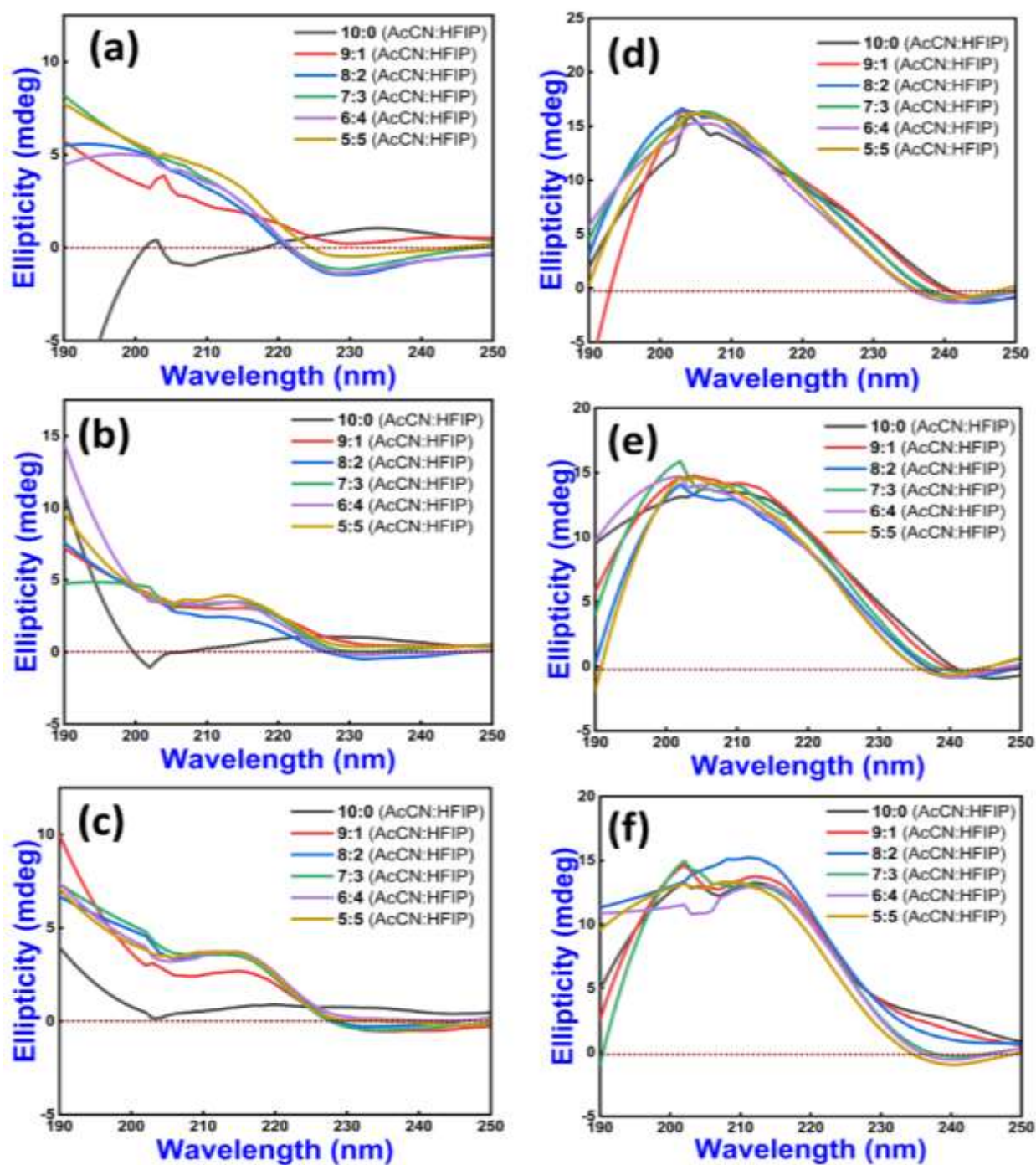
Fig. S19B. Circular Dichroism (CD) spectra of **1** (a), **2** (b), **3** (c) and **1-**Zn(II) (d), **2-**Zn(II) (e), **3-**Zn(II) (f), in different solvent combination of Acetonitrile and Hexafluoro isopropanol (HFIP) (AcCN:HFIP; v/v, 10:0 (Black line), 9:1 (Red line), 8:2 (Blue line), 7:3 (Green line), 6:4 (Voilet line), 5:5 (Yellow line)). Figure shown CD spectra between 190 nm to 250nm.
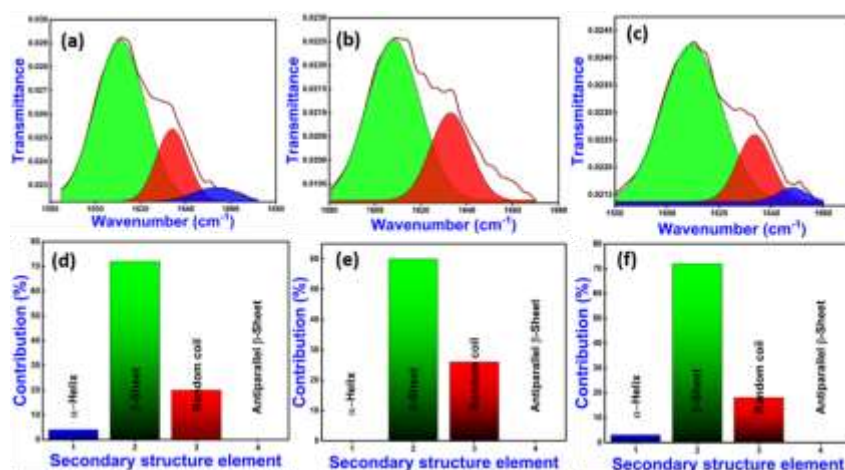
Fig. S20 A. (a) IR spectra of **1** (brown line) and deconvoluted plot (colour fill area), (d) Contributions of Secondary structure in self-assembly of **1**. (b) IR spectra of **2** (brown line) and deconvoluted plot (colour fill area), (e) Contributions of Secondary structure in self-assembly of **2**, (c) IR spectra of **3** (brown line) and deconvoluted plot (colour fill area), (f) Contributions of Secondary structure in self-assembly of **3**, IR Deconvolution plot in amide region 1580 to 1680 cm^{-1} by fitting multiple Gaussian peaks.
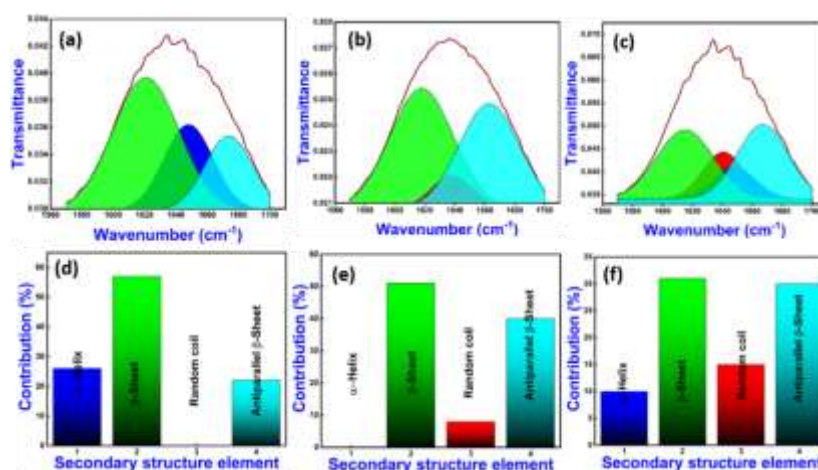
Fig. S20 B. (a) IR spectra of **1-**Zn(II) (brown line) and deconvoluted plot (colour fill area), (d) Contributions of Secondary structure in self-assembly of **1-**Zn(II). (b) IR spectra of **2-**Zn(II) (brown line) and deconvoluted plot (colour fill area), (e) Contributions of Secondary structure in self-assembly of **2-**Zn(II), (c) IR spectra of 3-Zn(II) (brown line) and deconvoluted plot (colour fill area), (f) Contributions of Secondary structure in self-assembly

of **3-**Zn(II), IR Deconvolution plot in amide region 1570 to 1700 cm^{-1} by fitting multiple Gaussian peaks.
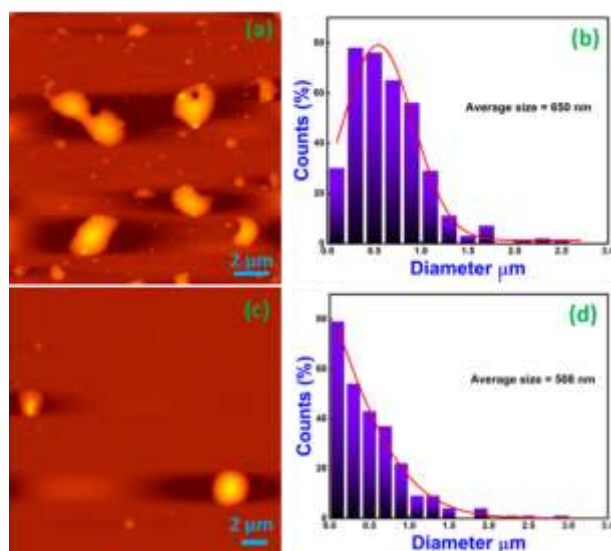
Fig. S21 AFM images (a) 2D self-assembly representation of **1**, (b) its corresponding particle size distribution histogram plot, (c) 2D self-assembly representation of **1-**Zn(II) complex, (d) its corresponding particle size distribution histogram plot.
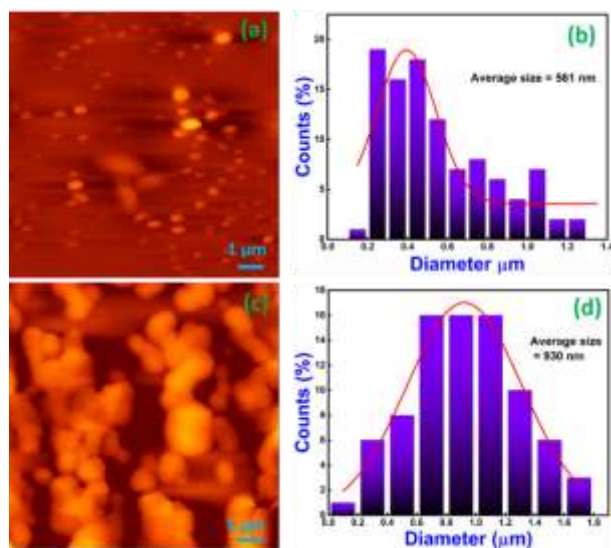
Fig. S22 AFM images (a) 2D self-assembly representation of **2**, (b) its corresponding particle size distribution histogram plot, (c) 2D self-assembly representation of **2-**Zn(II) complex, (d) its corresponding particle size distribution histogram plot.
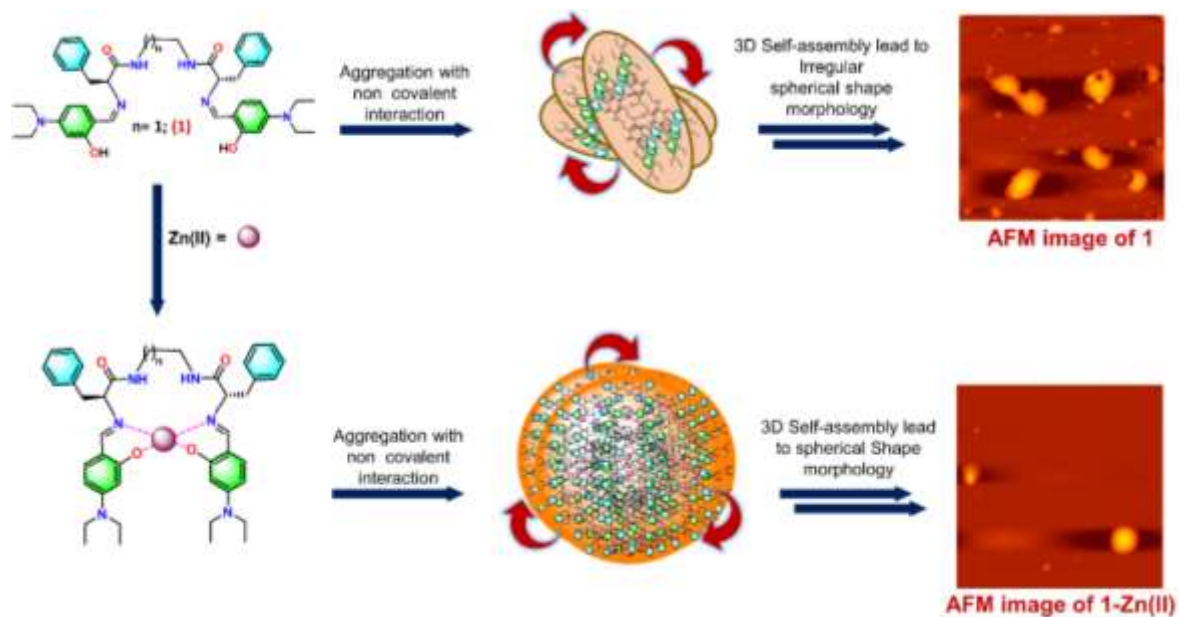
Scheme. S1. A Proposed model of change in self-assembly of **1** by addition of Zn(II) ions through 2D AFM image.
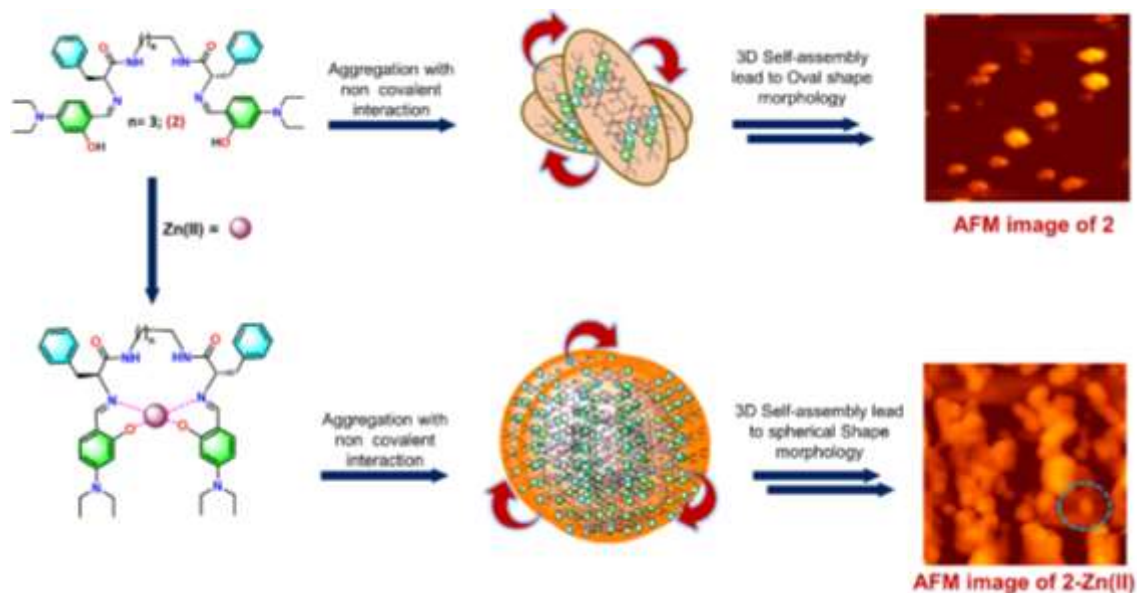
Scheme. S2. A Proposed model of change in self-assembly of **2** by addition of Zn(II) ions through 2D AFM image.

Table S1 Quantum yield of neat pseudopeptide **1-3** with and without Zn(II) ions.

S.No	Entry	Quantum yield
1	1	0.03
2	1+Zn(II)	0.08
3	2	0.02
4	2+Zn(II)	0.08
5	3	0.03
6	3+Zn(II)	0.13

Table S2 Fluorescence decay parameters of **1-3** in ethanol-water with and without Zn(II).

S.No.	Entry	(A)	τ (ns)	$<\tau>$ (ns)
1	1	0.54371 (A$_1$)	0.72118 (τ_1)	
2		0.16398 (A$_2$)	3.02126 (τ_2)	1.2540
3	1+Zn(II)	0.54469 (A$_1$)	0.80282 (τ_1)	
4		0.14668 (A$_2$)	3.3778 (τ_2)	1.3490
5	2	0.52808 (A$_1$)	0.64934 (τ_1)	
6		0.16273 (A$_2$)	3.06204 (τ_2)	1.2175
7	2+Zn(II)	0.53946 (A$_1$)	0.79712 (τ_1)	
8		0.14086 (A$_2$)	3.55353 (τ_2)	1.3677
9	3	0.52793 (A$_1$)	0.79482 (τ_1)	
10		0.09562 (A$_2$)	3.70187 (τ_2)	1.2404

11	**3**+Zn(II)	0.56368 (A_1)	1.18114 (τ_1)	
12		0.06995 (A_2)	6.61995 (τ_2)	1.7814

Dynamic parameters determined from $A_1\exp(-x/\tau_1) + A_2\exp(-x/\tau_2) + y_0$

The weighted mean lifetime $<\tau>$ was calculated by using following equation:

$<\tau> = (A_1\tau_1 + A_2\tau_2) / (A_1 + A_2)$

where, A_1/A_2 and τ_1/τ_2 are the fractions (A) and lifetimes (τ) respectively.

Solution concentration = 10 µM.

Apparatus and Materials

NMR (^{1}H and ^{13}C) spectra were performed in solvent $CDCl_3$ on a JEOL 500 FT-NMR at 500 MHz and 126 MHz respectively. HRMS experiments were studied on SCIEX X500R (QTOF-MS) mass spectrometer whereas, UV-Visible and fluorescence spectroscopy were recorded on Agilent Cary 60 UV-Visible with serial no.-MY19329220 single beam UV-Visible spectrometer and Fluoromax 4CP plus spectrofluorometer respectively by using a 10 mm quartz cuvette at room temperature. Time-resolved Photoluminescence (TRPL) spectroscopy were performed on laser-pulse diole laser with model number WITEC alpha 300 focus innovation (power = 0.250 mW). Circular Dichroism (CD) spectra of all compounds were performed on JASCO J-1500-450 at room temperature with serial no. D062161638 and Power A C 220V 50/60HZ 770VA with quartz cuvette (4ml, path length 1cm) and all CD spectrum were recorded in the 190 nm to 400 nm range.

Sample preparation of CD Experimet

Sample **1-3** were dissolved in acetonitrile (10^{-3} M) and zinc nitrate salt in distilled water (10^{-2} M) respectively. The experiment was performed in solvent mixture of Acetonitrile (AcCN) and Hexafluoro isopropanol (HFIP) in different ratio (AcCN:HFIP; 10:0, 9:1, 8:2, 7:3, 6:4, and 5:5) with same concentration (10^{-5}M).

All materials were procured from a commercial supplier and used it as received. *Z-L-*Phenylalanine amino acid was procured from SRL while HBr\ Acetic Acid, 4-(Diethylamino)salicylaldehyde, DCC, N-Hydroxysuccinimide, and all aliphatic diamine were procured from Sigma-Aldrich, India. Several metal salt such as, $AgNO_3$, $Cd(NO_3)_2 \cdot 4H_2O$, $Co(NO_3)_2 \cdot 6H_2O$, $Cu(NO_3)_2 \cdot 3H_2O$, $Ni(NO_3)_2 \cdot 6H_2O$, $Fe(NO_3)_3 \cdot 9H_2O$, $Pb(NO_3)_2$, $Ca(NO_3)_2 \cdot 4H_2O$, $Zn(NO_3)_2$, KNO_3, $Hg(NO_3)_2$, and $NaNO_3$ were procured from Himedia.

Atomic force microscopy (AFM) analysis

AFM study was performed to explore the structural morphology of **1-3** using NT-MDT with model no. Solver next. Freshly prepared sample **1-3** (with and without Zn(II)) at 10^{-5} M concentration of pure ethanolic solution and 5-10 µl aliquots of this sample was drop cast as a thin film on cover slip (glass sheet). The sample was dried for 10-12 hr. in dust free environment using vacuum desiccator. The number of partical from AFM image is calculated by using Nova Px_3.4 software by using the grain analysis tool.

FT-IR Spectroscopy

All FT-IR spectra of compound were performed on JASCO FT/IR-4700 by using KBr pellet, whereas for IR deconvolution study, all IR spectra were taken in liquid state. For sample preparation, neat compound **1-3** were dissolved in Acetonitrile (10^{-3} M), while **1-3** with

Zn(II) ion were prepared in mixture of Acetonitrile and water (10^{-3} M). The IR spectra in amide region I were fitted by multiple Gaussian peak and secondary structure contribution calculated through OriginPro 2021 software.

Experimental details

General method for optical measurement

For the study of photophysical measurement of **1-3** (10µM), the stock solution was prepared in HEPES buffer (Water:Ethanol = 3:7 v/v, 10µM; pH ~ 7.4) at room temperature and all metal ion solutions (Ag(I), Ca(II), Cd(II), Co(II), Cu(II), Fe(III), Hg(II), K(I), Na(I), Ni(II), Pb(II), and Zn(II)) were prepared by dissolving their nitrate salts in distilled water (10 mM). In the titration study, metal ions solution was added portion-wise in a 3.0 ml solution of **1-3** (10 µM) in quartz cuvette (4ml, path length 1cm).

Synthesis and characterization

Synthesis of 1: (2S,2'S)-N,N'-(ethane-1,2-diyl)bis(2-(((E)-4-(diethylamino)-2-hydroxybenzylidene)amino)-3-phenylpropanamide) Compound **A-C** were synthesised by following literature procedures.[1] The synthetic route of pseudopeptides **1-3** is illustrated in Scheme 1. Firstly, Compound **A** (708 mg, 2 mmol) was dissolved in 10 ml of dry ethanol; after a clear transparent solution was formed, it was added to 10 ml of dry Ethanolic solution of 4-(Diethylamino)salicylaldehyde (772 mg, 4 mmol) drop wise at 90°C. The resulting solution mixture was refluxed for 4-5 hr., and after completing the reaction, evaporate the solvent through rotavapor. The final product was washed through n-hexane multiple times, and we obtained desired product. Yield (1.155 g, 1.63 mmol, 82%); M.P. 77°C; IR (KBr pellet): 3411, 3296, 3062, 3026, 2971, 2927, 2871, 1659, 1633 cm^{-1}; ^{1}H NMR (500 MHz, CDCl$_3$, 23°C, TMS) δ 7.65 (s, 2H), 7.23 – 7.13 (m, 10H), 6.83 (d, J = 8.5 Hz, 2H), 6.56 (s,

2H), 6.13 (s, 2H), 6.11 (s, 2H), 3.90 – 3.88 (m, 2H), 3.35 – 3.30 (m, 14H), 3.01 (dd, J = 13.5, 9.5 Hz, 2H), 1.15 (t, J = 7.0 Hz, 12H); ^{13}C NMR (126 MHz, CDCl$_3$, 23°C, TMS) δ 172.82, 166.44, 163.05, 151.68, 137.91, 133.58, 129.95, 128.39, 126.58, 108.13, 103.50, 97.75, 75.02, 44.64, 41.03, 39.61, 12.78. HRMS (ESI-TOF) m/z: [M + H]$^+$ calcd for C$_{42}$H$_{53}$N$_6$O$_4$, 705.4123; found, 705.4124.

Synthesis of 2: (2S,2'S)-N,N'-(butane-1,4-diyl)bis(2-(((E)-4-(diethylamino)-2-hydroxybenzylidene)amino)-3-phenylpropanamide) This compound was obtained as described above and starting from **B** (765 mg, 2 mmol) and 4-(Diethylamino)salicylaldehyde (772 mg, 4 mmol); Yield (1.230g, 1.67 mmol, 84%); M.P. 70°C; IR (KBr pellet): 3402, 3297, 3061, 3028, 2970, 2930, 2872, 1651, 1622 cm^{-1}; ^{1}H NMR (500 MHz, CDCl$_3$, 23°C, TMS) δ 7.72 (s, 2H), 7.23 – 7.14 (m, 10H), 6.88 (d, J = 8.5 Hz, 2H), 6.30 (s, 2H), 6.15 (s, 2H), 6.13 (s, 2H), 3.94 (dd, J = 7.0, 1.5 Hz, 2H), 3.35 – 3.30 (m, 10H), 3.24 – 3.21 (m, 2H), 3.17 – 3.15 (m, 2H), 3.07 (dd, J = 13.0, 8.5 Hz, 2H), 1.40 – 1.34 (m, 4H), 1.17 – 1.14 (m, 12H); ^{13}C NMR (126 MHz, CDCl$_3$, 23°C, TMS) δ 171.79, 166.04, 163.29, 151.74, 137.57, 133.59, 129.90, 128.34, 126.56, 107.96, 103.58, 97.62, 74.45, 44.59, 41.03, 38.97, 26.76, 12.70. HRMS (ESI-TOF) m/z: [M + H]$^+$ calcd for C$_{44}$H$_{57}$N$_6$O$_4$, 733.4436; found, 733.4419.

Synthesis of 3: (2S,2'S)-N,N'-(hexane-1,6-diyl)bis(2-(((E)-4-(diethylamino)-2-hydroxybenzylidene)amino)-3-phenylpropanamide). This compound was obtained as described above and starting from **C** from (850 mg, 2 mmol) and 4-(Diethylamino) Salicylaldehyde (772 mg, 4 mmol);. Yield (1.262g, 1.65 mmol, 83%,); M.P. 96°C; IR (KBr pellet): 3418, 3208, 3060, 3027, 2972, 2931, 2867, 1659, 1634 cm^{-1}; ^{1}H NMR (500 MHz, CDCl$_3$, 23°C, TMS) δ 7.71 (s, 2H), 7.23 – 7.14 (m, 10H), 6.88 (d, J = 8.5 Hz, 2H), 6.21 (s, 2H), 6.16 (d, J = 2.0 Hz, 2H), 6.14 (s, 2H), 3.92 (dd, J = 8.5, 3.5 Hz, 2H), 3.38 – 3.31 (m, 12H), 3.26 – 3.12 (m, 4H), 3.08 (dd, J = 13.5, 8.5 Hz, 2H), 1.42 – 1.38 (m, 4H), 1.21 – 1.16 (m, 16H); ^{13}C NMR (126 MHz, CDCl$_3$, 23°C, TMS) δ 171.74, 166.15, 163.04, 151.67,

137.70, 133.54, 129.96, 128.38, 126.61, 108.05, 103.58, 97.63, 74.87, 44.66, 41.17, 39.27, 29.40, 26.42, 12.76. HRMS (ESI-TOF) m/z: $[M + H]^+$ calcd for $C_{46}H_{61}N_6O_4$, 761.4749; found, 761.4758.

Refrences:

1. J. Becerril, M. Bolte, M. I. Burguete, F. Galindo, E. García-España, S. V. Luis and J. F. Miravet, *J. Am. Chem . Soc.,* 2003, **125**, 6677–6686.